Negative Snakes in JET: Evidence for Negative Shear?

R D Gill, B Alper, A W Edwards, D Pearson[1].

JET Joint Undertaking, Abingdon, Oxon, OX14 3EA.
[1] Present address: University of Reading, UK.

INTRODUCTION Snakes have been observed in many tokamaks as a novel form of MHD activity which consists of a long lived small region of high electron pressure on the $q = 1$ magnetic surface. They have a $m = n = 1$ topology and are often formed during the injection of solid pellets of D_2 [1] which reach in to the $q = 1$ surface. Snakes have also been observed [2], at the onset of sawtoothing, after neutral beam heating of the plasma centre, and in discharges with rather flat central profiles of electron density and pressure. The name "snake" arises from their characteristic appearance when observed by a soft X-ray camera.

A detailed analysis of the soft X-ray data together with the electron density (n_e) and temperature (T_e) information from the interferometer and ECE systems respectively has shown that the pellet induced snakes typically have perturbed parameters relative to their surroundings of $\delta n_e / n_e \sim 25$ to 140% and $\delta T_e \sim 0$ to 200eV. Generally, pellet induced snakes have no visible temperature perturbations at times greater than 100ms after their creation. In discussing the properties of the snakes it is useful to write simplified expressions for the plasma radiated X-ray power (P_x) and the plasma resistivity (R)

$$P_x = A n_e^2 \zeta f(T_e) \quad \text{and} \quad R = B \frac{Z_e}{T_e^{3/2}}$$

where ζ is the X-ray anomaly factor and f (T_e) is a function of temperature which, for the particular filters placed between the plasma and the detectors, is proportional to T_e^{α} with $\alpha \approx 1$. The plasma effective charge Z_e is approximately proportional to ζ, and A and B are constants. Small perturbations within the snake may therefore be written as

$$\frac{\delta P_x}{P_x} = 2\frac{\delta n_e}{n_e} + \frac{\delta\zeta}{\zeta} + \frac{\delta T_e}{T_e} \quad \text{and} \quad \frac{\delta R}{R} = \frac{\delta Z_e}{Z_e} - \frac{3}{2}\frac{\delta T_e}{T_e} \approx \frac{\delta\zeta}{\zeta} - \frac{3}{2}\frac{\delta T_e}{T_e}.$$

The perturbed impurity concentration within the snake is generally not known. However, $\delta R/R$ maybe obtained by eliminating $\delta\zeta/\zeta$. A detailed analysis [2] has shown that at early times in the pellet snake's lifetime $\delta R/R$ is positive because of the reduced T_e, whereas on longer timescales $\delta T_e/T_e \sim 0$ but $\delta\zeta/\zeta > 0$ which also leads to an enhanced resistivity in the snake. The association of the snake with a reduced temperature or enhanced impurity concentration leads to the idea that it is formed by a magnetic island with the locally changed parameters producing a region of increased resistivity and decreased current density. This is particularly plausible for pellet injection as the stagnation of the cold particles on the $q = 1$ surface would produce, on a short timescale, a region of very much reduced T_e.

NEGATIVE SNAKES Occasional observations have been made in JET of so-called negative snakes. A typical example is shown in Fig. 1 where data from the 38 channel vertical soft X-ray camera is displayed. The signature of these from the soft X-ray cameras is very similar to the more usual snakes except that the localised region of the snake has, compared with its surroundings, decreased rather than increased emission. Negative snakes have been seen under the following circumstances. (i) Between sawteeth in low-q discharges with I_p = 3.3 - 7MA. (ii) As successor oscillations following a sawtooth crash. (iii) Immediately after pellet injection. The first type of negative snake is shown in Fig. 1 for a discharge with I_p = 7MA.

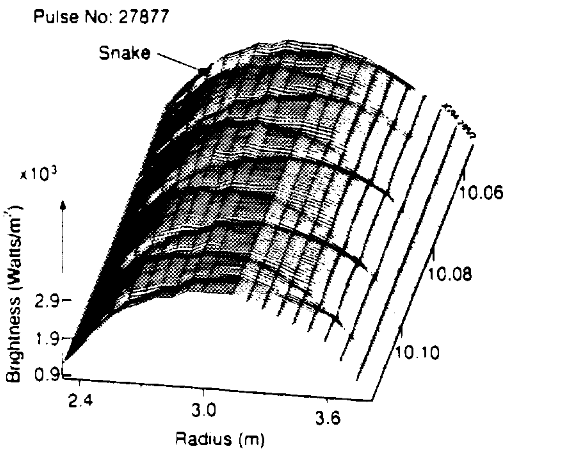

Fig. 1: Line integrated soft X-ray emission observed by the vertical soft X-ray camera showing the negative snake.

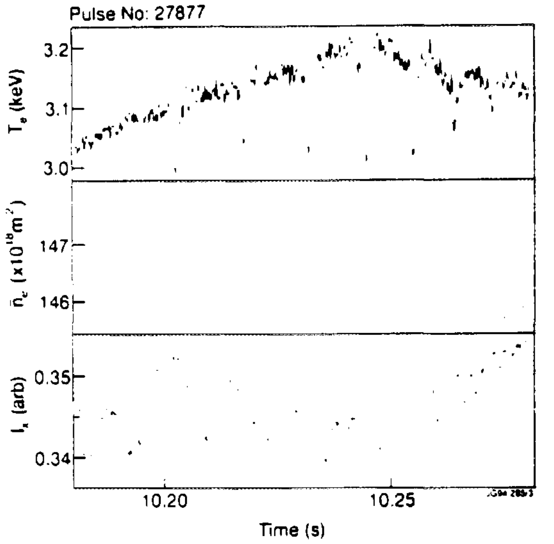

Fig. 2: The traces shown are T_e at R = 3.67m, the electron density line integrated along a central vertical chord and a line integrated soft X-ray signal.

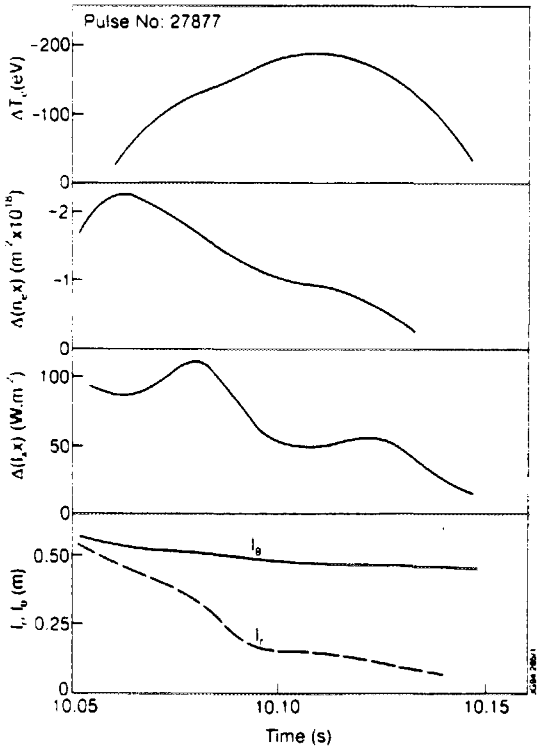

The interpretation of these negative snakes has always been difficult due to the lack of detailed measurements of n_e and T_e profiles. It had always been assumed that the negative snakes had a very similar structure to the normal snakes. However the detailed n_e and T_e measurements (Fig. 2) show a different picture. The variation of various parameters for the negative snake are collected in Fig. 3 and in Table 1 the negative snakes are

Fig. 3: The time variation is shown for various negative snake parameters. The variations of T_e, the line integrated n_e and line integrated X-ray intensity are shown in the upper part of the figure. The radial and poloidal dimension are also shown.

Table 1

$\frac{\delta P_x}{P_x}$(%)	$\frac{\delta n_e}{n_e}$(%)	$\frac{\delta T_e}{T_e}$(%)	ℓ_r (m)	ℓ_θ (m)	
-8	-10	-3·3	0.41	0.52	} - ve snake early
-15	-13	-5·4	0.11	0.47	} - ve snake late
+150	+140	-22	0.14	0.25	} Pellet snake early
+100	+40	< 5	0.20	0.25	} Pellet snake late

contrasted with pellet induced snakes. The radial and poloidal dimensions of the snake are ℓ_r and ℓ_θ. From the figure it may be seen that the shape of the negative snake varies from nearly circular to a shape with only a small radial extent. The figures in the table can be used to show that $\delta R/R \sim 20$ - 25% i.e. that the negative snake is a region of increased resistance and, as $\delta\zeta/\zeta = 13$ - 16%, also a region of increased impurity density. In these respects the negative snakes are similar to normal snakes. However, contour plots of the ECE data show quite a different picture. In these measurements T_e is determined along a minor radius in the outer half of the median plane. The rotation of the plasma makes it possible to produce a pseudo-contour plot over the entire structure of the snake. These plots (Fig. 4) clearly show that the negative snake sits at the X-point of the island structure. If the temperature is plotted normalised to the average temperature at a particular radius then the more familiar localised picture of the snake appears (Fig. 5). The other prominent feature of the temperature profile is its hollowness. The negative snakes are in fact sitting on the rim of a volcano shaped structure.

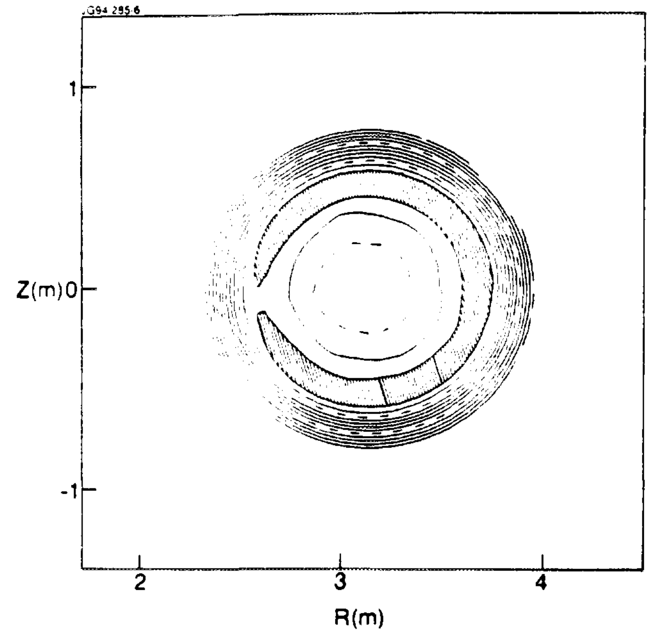

Fig. 4: Contour plot of T_e.

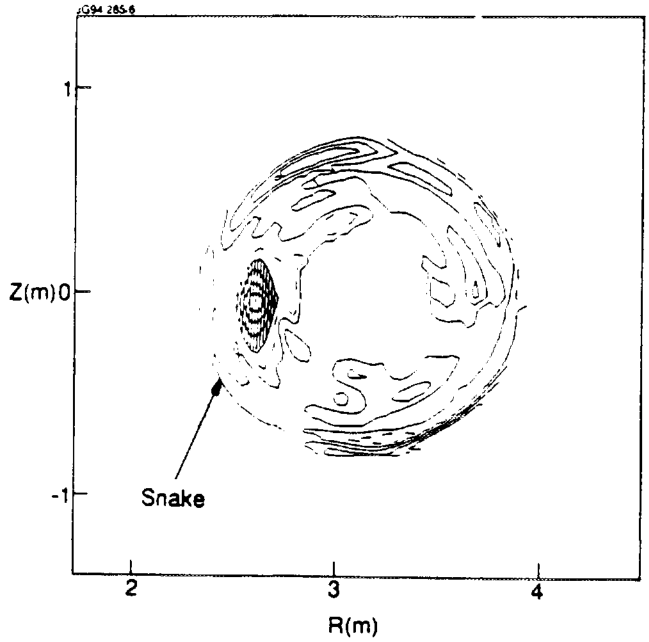

Fig 5: Contour plot of T_e normalised to the average temperature $\langle T_e \rangle$ at a particular minor radius.

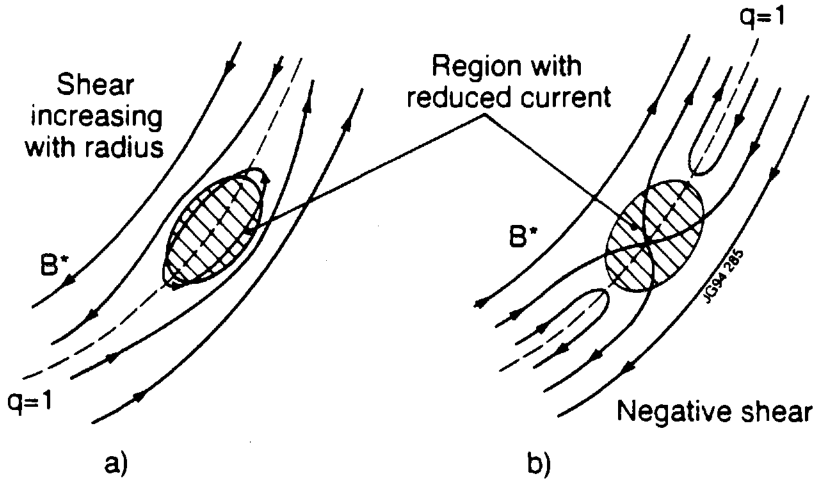

Fig. 6: Magnetic field structure with (a) positive shear and (b) negative shear.

EFFECTS OF SHEAR In the case of normal snakes, the effect of substantial plasma cooling by the pellet injection was convincingly argued to be a cause of magnetic island formation which then became identified with the snake. These calculations assumed a "normal" q-profile that increased with minor radius. Further theoretical work [3] showed that the bootstrap current could explain several of the observed features of the snake. The relationship between the shear and the current pertubation is shown schematically in fig. 6 where the magnetic poloidal field, $B^* = B_\theta\ (1\text{-}q)$, in helical coordinates is shown in the region of the q=1 surface. If q increases with radius then B* is in the same direction as B_θ within the q=1 surface and reversed outside it. A locally reduced current density will form an island as shown in fig. 6a. However, as the negative snakes have a locally reduced current density and sit at the X-point of the island structure it seems to be an inescapable conclusion that the magnetic shear is reversed at the point of the snake, i.e. that q is decreasing with radius, as shown in fig. 6b. This could be possible in these particular discharges as the electron temperature profiles are generally hollow except just for the time before the sawtooth collapse where the snakes in any case disappear. It would therefore appear that the q-profile in these low q-discharges is different from what might have been expected, but other instances of unusual q-profile have been observed in JET in PEP discharges [4], hot ion H-modes [5], and counter-injection [6] heated discharges.

REFERENCES.

[1] A. Weller et al., Phys. Rev. Lett., 59 (1987) 2303.

[2] R.D. Gill et al., Nuclear Fusion, 32 (1992) 723.

[3] A. Thyagaraja and F.A. Haas, Phys. Fluids., B5 (1993) 3252.

[4] M. Hugon et al., Nuclear Fusion, 32 (1992) 33.

[5] M.F.F. Nave et al., submitted to Nuclear Fusion.

[6] A. Edwards et al., 1992 Int. Conf. on Plas. Phys. (Innsbruck) 16C, Part 1, 379.